

# Prediction of optical coherence tomography-detected calcified nodules using coronary computed tomography angiography

**Junichi Sugiura**

Nara Medical University

**Makoto Watanabe** (✉ [wmakoto07@kcn.jp](mailto:wmakoto07@kcn.jp))

Nara Medical University

**Saki Nobuta**

Nara Medical University

**Akihiko Okamura**

Nara Medical University

**Atsushi Kyodo**

Nara Medical University

**Takuya Nakamura**

Nara Medical University

**Kazutaka Nogi**

Nara Medical University

**Satomi Ishihara**

Nara Medical University

**Yukihiro Hashimoto**

Nara Medical University

**Tomoya Ueda**

Nara Medical University

**Ayako Seno**

Nara Medical University

**Kenji Onoue**

Nara Medical University

**Tsunenari Soeda**

Nara Medical University

**Yoshihiko Saito**

Nara Medical University

**Keywords:** Calcified nodule, optical coherence tomography, coronary computed tomography, percutaneous coronary intervention

**Posted Date:** August 8th, 2022

**DOI:** <https://doi.org/10.21203/rs.3.rs-1903762/v1>

**License:**  This work is licensed under a Creative Commons Attribution 4.0 International License.

[Read Full License](#)

---

# Abstract

Diagnosis of Calcified nodules (CNs) is critical in proper management of coronary artery disease but CNs can be detected only using intracoronary imaging modalities. This study aimed to investigate the ability of coronary computed tomography angiography (CCTA) in predicting CNs detected by optical coherence tomography (OCT). In total, 138 patients (249 vessels) who underwent OCT after CCTA evaluation were retrospectively enrolled and classified into CN (11 patients / 12 vessels) and non-CN (127 patients / 237 vessels) groups based on the OCT analysis. Retrospective CCTA analysis revealed that coronary artery calcification score (CACS), calcified plaque volume (CPV), non-calcified plaque volume (NCPV), low-attenuation plaque volume (LAPV), and maximum calcified plaque area (MCPA) in the target vessel were significantly larger in the CN group than in non-CN group. Receiver operating characteristic curve indicated that  $CACS \geq 162$  (area under the ROC curve (AUC) 0.86, sensitivity 83.3%, specificity 71.3%),  $CPV \geq 20.2 \text{ mm}^3$  (AUC 0.88, sensitivity 91.7%, specificity 70.5%),  $NCPV \geq 1737 \text{ mm}^3$  (AUC 0.71, sensitivity 75.0%, specificity 72.6%),  $LAPV \geq 358 \text{ mm}^3$  (AUC 0.71, sensitivity 91.7%, specificity 52.7%), and  $MCPA \geq 4.51 \text{ mm}^2$  (AUC 0.9, sensitivity 91.7%, specificity 84.0%) were the best cutoff value for predicting CNs. Therefore, CCTA is useful for predicting OCT-detected CNs.

## Introduction

Calcified nodules (CNs), which are protrusions into the blood vessel lumens, are pathologically associated with acute coronary syndrome (ACS)[1–3] and other major cardiovascular events, such as target lesion revascularization, stent thrombosis, and myocardial infarction (MI) after percutaneous coronary intervention (PCI)[4, 5]. The diagnosis of CNs is critical in proper management of patients with coronary artery disease. At present, invasive intracoronary imaging modalities, such as intravascular ultrasound (IVUS) and optical coherence tomography (OCT), are generally implemented for the in vivo diagnosis of CNs, but non-invasive methods are lacking.

Coronary computed tomography angiography (CCTA) is a noninvasive tool for evaluating the coronary plaque morphology; coronary plaques can be classified on the basis of computed tomography (CT) values as low-attenuation, fibrous, and calcified plaques, with quantitative assessment of plaque volumes[6–8]. CCTA-calculated coronary artery calcium score (CACS) is widely used to quantitatively evaluate the coronary artery calcium burden[9], where a higher CACS is related to poorer clinical outcomes as compared with lower CACS[10, 11].

OCT is an intravascular imaging modality with a maximal spatial resolution of 10  $\mu\text{m}$ , which is 10-fold higher than that of IVUS[12, 13]. Because near-infrared light from the OCT system can penetrate calcium, OCT provides a more detailed characterization of the morphology of calcified coronary plaques as compared with IVUS[14, 15]. Several studies employing OCT have reported that CNs are frequently observed in lesions with large amounts of calcified plaques[5, 16, 17]. Since CCTA quantitatively evaluates calcium plaques, estimation of coronary calcium burden by CCTA may help identify the

presence of CNs. This study aimed to investigate the diagnostic ability of CCTA to identify CNs in patients undergoing PCI.

## Materials And Methods

### Study population

This single-center, retrospective, and observational study was conducted at Nara Medical University, Japan. A total of 341 patients who underwent OCT-guided PCI for de novo target vessels after CCTA evaluation between January 2014 and December 2018 were screened. Patients with any of the following conditions were excluded from the study: (1) ST elevation or non-ST elevation MI, (2) vessels with PCI before CCTA evaluation, (3) > 1 year duration between CCTA and OCT, (4) absence of OCT images before stent implantation, and (5) unanalyzable CCTA or OCT images. Finally, 138 patients (249 vessels) were included and classified (based on OCT analysis) into the following two groups: (1) CN group, 11 patients (12 vessels) with OCT-detected CNs and (2) non-CN group, 127 patients (237 vessels) (Fig. 1). Patient characteristics were collected from the medical records, while the results of blood investigations conducted within 3 months of OCT were analyzed.

This study was approved by the Ethics Committee of Nara Medical University (reference no. 1759-2) and complied with the Declaration of Helsinki's ethical principles. Informed consent was obtained in the form of an opt-out option from the Department of Cardiovascular Medicine, Nara Medical University website.

### Ccta Procedure And Analysis

CCTA was performed using a dual-source CT scanner (Somatom Definition, Siemens, Forchheim, Germany). The detailed scan protocol is described in **Supplementary materials**. CCTA analysis was performed using the SYNAPSE VINCENT version 5.1. Images were independently evaluated by 3 investigators familiar with the CCTA analysis, and any disagreements were resolved by consensus. Retrospective CCTA studies were performed for each vessel evaluated with OCT. Coronary plaques were defined as structures with a minimum 1 mm<sup>2</sup> area within or adjacent to the arterial lumen, clearly distinguishable from the vessel lumen, and surrounded by pericardial tissue; tissue with signal intensity below -30 Hounsfield units (HU) was considered pericardial fat and excluded from the analysis. Based on the results of our previous study with OCT[7–9], each tissue was classified by its CT value (< -30, -30 to 50, 51 to 200, 201 to 500, and > 500 HU indicated pericardial fat, low-attenuation plaque, fibrous plaque, enhanced media, and calcified plaque, respectively). Non-calcified plaques were defined as low-attenuation or fibrous plaques. Previous studies have reported that high-risk plaque features, such as positive remodeling (a lesion with a remodeling index of  $\geq 1.1$ ), very low-attenuation plaque (minimum CT value of  $\leq 30$  HU), napkin-ring sign (a central low-attenuation portion surrounded by a ring-like higher attenuation), and spotty calcifications (a small calcification of 3 mm or less on curved multiplanar

reformation images and occupying only one side on the cross-sectional images) are predictive factors for cardiac events[8, 18–20].

First, each vessel was classified into four segments (right coronary artery, left main trunk, left anterior descending, and left circumflex). Each segment vessel was evaluated for the CACS (evaluated using the Agatston score[17]), calcified plaque volume (CPV; in  $\text{mm}^3$ ), non-calcified plaque volume (NCPV;  $\text{mm}^3$ ), low-attenuation plaque volume (LAPV;  $\text{mm}^3$ ), fibrous plaque volume ( $\text{mm}^3$ ), maximum calcified plaque area (MCPA) on the cross-sectional images ( $\text{mm}^2$ ), and presence of positive remodeling, very low-attenuation plaque, napkin-ring sign, and spotty calcifications. MCPA was measured at the largest calcified plaque area on cross-sectional measurements at 1-mm intervals through the entire target vessel. Volumetric assessment for each classified plaque (calcified plaque, non-calcified plaque, low-attenuation plaque, and fibrous plaque) by CT value was completed automatically with SYNAPSE VINCENT version 5.1.

## OCT study and analysis

OCT imaging was performed using a frequency-domain OCT system (C8 System, Dragonfly Imaging Catheter and ILUMIEN OPTIS; St. Jude Medical, St. Paul, MN, USA) or an optical frequency-domain imaging (OFDI) system (Terumo, Tokyo, Japan). The OCT imaging technique has been previously described[21].

An OCT examination was performed for the PCI target vessel as distally as possible before PCI to evaluate the morphology of the calcified plaque. For lesions with severe narrowing precluding passage of the OCT or OFDI catheter, removal of blood from the field for clear visualization of the vessel wall, or lesions with an angiographically visible thrombus, the baseline OCT examination was performed after pre-dilatation using a balloon catheter, rotational atherectomy, or thrombectomy.

A calcified plaque is defined as a low-signal intensity area with sharply delineated borders[5, 22]. OCT-detected CN was defined as a high-backscattering mass protruding into the lumen with the strong signal attenuation and irregular surface[5, 22]. Representative OCT and CCTA images of calcified plaques are shown in Fig. 2.

The OCT images were analyzed by two independent observers (S.I. and M.W.) in a blinded manner using a dedicated offline review system (St. Jude Medical). Two observers blinded to each patient's clinical and lesion characteristics independently performed the OCT measurements. Any discordance between the two observers was resolved by consensus with a third reviewer (A.O.).

## Statistical analysis

Depending on the distribution, categorical and continuous variables were represented as numbers/percentages and means  $\pm$  standard deviations or medians/interquartile ranges, respectively. Student's t-test and Wilcoxon test were performed to examine the nominal variables and continuous values with normal and non-normal distributions, respectively. Further, the nominal variables were also

examined using the Fisher's exact test. Receiver operating characteristic (ROC) curve analysis and area under the ROC curve (AUC) were used to determine the best cutoff values for quantitative CCTA parameters for predicting the OCT-detected CNs. The best cutoff value was defined as the value with the highest sum of Youden's index (sensitivity + specificity - 1). Significant superiority tests were two-sided and *P* values < 0.05 were considered significant. JMP version 14 software (SAS Institute Inc., Cary, NC, USA) was used for statistical analysis.

## Results

Table 1 shows the patient characteristics and results of laboratory findings. Hypertension was significantly higher in the CN group than that of the non-CN group. Further, patients of the CN group were more frequently treated with maintenance dialysis and insulin than those of the non-CN group. Furthermore, significant differences were observed in the hemoglobin levels, estimated glomerular filtration rates, and products of calcium and phosphate levels between the two groups.

Table 1  
Baseline characteristics in patients with and without CN

	<b>CN group patients (n = 11)</b>	<b>Non-CN group patients (n = 127)</b>	<b>p value</b>
Age, years	70 ± 6	68 ± 10	0.54
Male sex, n (%)	8 (72.7)	102 (80.3)	0.56
Hypertension, n (%)	11 (100)	92 (72.4)	0.04
Dyslipidemia, n (%)	7 (63.7)	90 (70.9)	0.52
Diabetes mellitus, n (%)	6 (54.5)	57 (44.9)	0.77
Chronic kidney disease, n (%)	6 (54.5)	43 (33.9)	0.12
History of smoking, n (%)	8 (72.7)	102 (80.3)	0.72
Hemodialysis, n (%)	4 (36.4)	9 (7.1)	0.02
Prior myocardial infarction, n (%)	0 (0)	11 (8.7)	0.61
Prior stroke, n (%)	1 (9.1)	20 (15.8)	0.70
Peripheral arterial disease, n (%)	4 (33.3)	28 (11.8)	0.05
Medications at discharge, n (%)			
Antiplatelet therapy			0.56
Single antiplatelet therapy	2 (18.2)	26 (20.5)	
Dual antiplatelet therapy	8 (72.7)	75 (59.1)	
Oral anticoagulant			0.09
Warfarin	1 (9.1)	3 (2.4)	
Direct oral anticoagulant	1 (9.1)	9 (7.1)	
Statin	6 (54.5)	70 (55.1)	1.00
Ezetimibe	0 (0)	2 (1.6)	1.00
Oral hypoglycemic agents	3 (27.3)	41 (32.3)	0.76
Insulin	4 (36.4)	6 (4.7)	0.005
Laboratory findings			
Hemoglobin, g/dl	12.2 ± 1.3	13.7 ± 1.6	0.004
Values are presented as numbers (%), means ± standard deviations, or medians (interquartile ranges). CN, calcified nodule; eGFR, estimated glomerular filtration rate; HDL-C, high-density lipoprotein cholesterol; LDL-C, low-density lipoprotein cholesterol			

	<b>CN group patients (n = 11)</b>	<b>Non-CN group patients (n = 127)</b>	<b>p value</b>
Creatinine, mg/dl	1.06 (0.69–6.91)	0.88 (0.76–1.04)	0.21
eGFR, ml/minutes/1.73m <sup>2</sup>	46.1 (7.1–65.4)	65.4 (53.3–73.6)	0.04
HDL-C, mg/dl	49 ± 15	50 ± 14	0.84
LDL-C, mg/dl	92 ± 30	96 ± 30	0.62
Hemoglobin A1c, %	6.6 ± 0.9	6.3 ± 0.8	0.39
Calcium, mg/dl	9.1 ± 0.4	9.2 ± 0.4	0.5
Phosphate, mg/dl	3.7 ± 0.6	3.3 ± 0.6	0.07
Corrected calcium, mg/dl	9.1 ± 0.4	8.9 ± 0.5	0.32
Calcium-phosphate product	33.2 ± 5.8	29.5 ± 5.4	0.03
Values are presented as numbers (%), means ± standard deviations, or medians (interquartile ranges). CN, calcified nodule; eGFR, estimated glomerular filtration rate; HDL-C, high-density lipoprotein cholesterol; LDL-C, low-density lipoprotein cholesterol			

No significant difference was observed between the two groups for the duration from CCTA to OCT examination (CN group: 2 [interquartile range (IQR) 1 – 6] months; non-CN group: 1 [IQR 1 – 3] months:  $P=0.24$ ). The total CACS at the all coronary vessels was significantly ( $P<0.001$ ) higher in the CN group (1164 [IQR 802 – 2189]) than that in the non-CN group (308 [IQR 107 – 781]).

Table 2 shows a comparison of CCTA findings at the PCI target vessels between the CN and non-CN groups. Significant differences were observed between the CN- and non-CN groups in CACS (342 [IQR 203 – 855] vs. 49 [IQR 0 – 184]:  $P<0.0001$ ), CPV (77.4 mm<sup>3</sup> [IQR 29.3 – 212.8] vs. 2.1 mm<sup>3</sup> [IQR 0 – 24.1]:  $P<0.0001$ ), NCPV (1845 mm<sup>3</sup> [IQR 1410 – 2070] vs. 962 mm<sup>3</sup> [IQR 273 – 1870]:  $P=0.02$ ), LAPV (761 mm<sup>3</sup> [IQR 471–1059] vs. 290 mm<sup>3</sup> [IQR 92–709]:  $P=0.01$ ), and MCPA (8.12 mm<sup>2</sup> [IQR 5.32 – 12.30] vs. 0.02 mm<sup>2</sup> [IQR 0 – 30.5]:  $P<0.0001$ ). No significant differences were observed in the incidences of positive remodeling, very low-attenuation plaques, napkin-ring signs, and spotty calcification between the two groups.



Table 2  
CCTA findings at culprit vessel

	<b>CN group vessels (n = 12)</b>	<b>Non-CN group vessels (n = 237)</b>	<b>p value</b>
Coronary artery calcification score	342 (203–855)	49 (0-184)	< 0.0001
Calcified plaque volume, mm <sup>3</sup>	77.4 (29.3-212.8)	2.1 (0-24.1)	< 0.0001
Non-calcified plaque volume, mm <sup>3</sup>	1845 (1410–2070)	962 (273–1870)	0.02
Low attenuation plaque volume, mm <sup>3</sup>	761 (471–1059)	290 (92–709)	0.01
Fibrous plaque volume, mm <sup>3</sup>	964 (736–1470)	597 (178–1133)	0.06
Maximum calcified plaque area, mm <sup>2</sup>	8.12 (5.32–12.30)	0.02 (0-30.5)	< 0.0001
Positive remodeling, n (%)	2 (16.7)	15 (6.3)	0.19
Very low attenuation plaque, n (%)	0 (0)	29 (12.2)	0.37
Napkin-ring sign, n (%)	0 (0)	16 (6.8)	1.00
Spotty calcification, n (%)	0 (0)	41 (17.3)	0.23
Segment, n (%)			0.05
Right coronary artery	3 (25.0)	32 (13.5)	
Left main trunk	1 (8.3)	108 (45.6)	
Left anterior descending artery	7 (58.3)	71 (30.0)	
Left circumflex artery	1 (8.3)	26 (11.0)	
Values are presented as numbers (%) or medians (interquartile ranges). CCTA, coronary computed tomography angiography; CN, calcified nodule			

Figure 3 shows the ROC curve analysis for CCTA parameters to predict OCT-detected CNs. The optimal cutoff values to predict the presence of CNs were CACS  $\geq$  162 (AUC = 0.86), CPV  $\geq$  20.2 mm<sup>3</sup> (AUC = 0.88), NCPV  $\geq$  1737 mm<sup>3</sup> (AUC = 0.71), LAPV  $\geq$  358 mm<sup>3</sup> (AUC = 0.71), and MCPA  $\geq$  4.51 mm<sup>2</sup> (AUC = 0.9). Table 3 summarizes the diagnostic accuracies of CCTA parameters for predicting CNs. MCPA showed the highest AUC among all the CCTA parameters; however, no significant differences were observed in AUCs of MCPA and CACS or CPV (Table S1). Furthermore, AUCs of combinations of MCPA with other CCTA parameters did not yield improvements in CN predictions. All CCTA parameters showed negative predictive values (NPVs) of > 90%, but low positive predictive values (PPVs). Among all the CCTA parameters, the combination of MCPA ( $\geq$  4.51 mm<sup>2</sup>) and NCPV ( $\geq$  1737 mm<sup>3</sup>) showed the highest diagnostic accuracy (92.0%) and PPV (33.3%). Table 4 shows the CCTA findings of vessels with CNs. Eleven of the 12 vessels with CNs showed MCPA of  $\geq$  4.51 mm<sup>2</sup>. Moreover, all CNs were present within

the calcified plaques, including the cross-sectional slices with MCPA.  $CACS \geq 162$ ,  $CPV \geq 20.2 \text{ mm}^3$ , and  $MCPA \geq 4.51 \text{ mm}^2$  in the culprit vessel were the best cut-off values for discriminating CN

Table 3  
Diagnostic accuracy of CCTA parameters for predicting OCT-detected CN

	AUC	Accuracy (%)	Sensitivity (%)	Specificity (%)	PPV (%)	NPV (%)
$CACS \geq 162$	0.86	71.9	83.3	71.3	12.8	98.8
$CPV \geq 20.2 \text{ mm}^3$	0.88	71.5	91.7	70.5	13.6	99.4
$NCPV \geq 1737 \text{ mm}^3$	0.71	72.7	75.0	72.6	12.2	98.3
$LAPV \geq 358 \text{ mm}^3$	0.71	54.6	91.7	52.7	8.9	99.2
$MCPA \geq 4.51 \text{ mm}^2$	0.9	84.3	91.7	84.0	22.5	99.5
$MCPA \geq 4.51 \text{ mm}^2 + CACS \geq 162$	0.9	85.9	83.3	86.1	23.3	99.0
$MCPA \geq 4.51 \text{ mm}^2 + CPV \geq 20.2 \text{ mm}^3$	0.88	84.3	83.3	84.4	21.3	99.0
$MCPA \geq 4.51 \text{ mm}^2 + NCPV \geq 1737 \text{ mm}^3$	0.83	92.0	66.7	93.2	33.3	98.2
$MCPA \geq 4.51 \text{ mm}^2 + LAPV \geq 358 \text{ mm}^3$	0.87	89.2	83.3	89.5	28.6	99.1
CACS, coronary artery calcification score; CCTA, coronary computed tomography angiography; CN, calcified nodule; CPV, calcified plaque volume; LAPV, low-attenuation plaque volume; MCPA, maximum calcified plaque area; NCPV, non-calcified plaque volume; NPV, negative predictive value; PPV, positive predictive value						

Table 4  
CCTA findings in culprit vessels with CN

Vessel number	Segment	CACS	CPV, mm <sup>3</sup>	NCPV, mm <sup>3</sup>	LAPV, mm <sup>3</sup>	MCPA, mm <sup>2</sup>
1	LAD	347.44	33.87	1080	358	4.51
2	LMT	88.1	20.14	112	35	5.44
3	LAD	595.1	104.83	1912	1134	12.93
4	RCA	1828.5	462.97	3890	759	9.78
5	LCX	674.8	177.1	1737	763	9.47
6	LAD	309.7	224.76	1840	786	17.53
7	LAD	336.6	25.96	1789	835	5.28
8	LAD	193.9	39.4	1849	493	6.77
9	RCA	1339.5	255.76	2029	1690	21.77
10	LAD	161.9	27.71	2830	1227	2.14
11	RCA	914.5	127.7	2084	576	10.41
12	LAD	232	49.94	1301	464	5.68

CACS, Coronary artery calcified score; CCTA, coronary computed tomography angiography; CN, calcified nodule; CPA, calcified plaque area; CPV, calcified plaque volume; LAD, left anterior descending; LAPV, low attenuation plaque volume; LCX, left circumflex; LMT, left main trunk; MCPA, maximum calcified plaque area; NCPV, non-calcified plaque volume; RCA, right coronary artery

## Discussion

Non-invasive methods for the diagnosis of CNs, which are among the causative factors for ACS, are not available; this study investigated the possibility of using CCTA, a quantitative method of evaluating the calcium burden in vessels, in predicting the presence of CNs by analyzing patients who underwent OCT-guided PCI. The results indicate that CCTA-driven quantitative evaluation of the calcified plaques may be advantageous for predicting OCT-detected CNs.

CCTA-measured CACS is widely used for the quantitative evaluation of calcium burden[9] and prediction of coronary events[10, 11], and is calculated based on regions with CT values  $\geq 130$  HU[9]. On the other hand, CPV is calculated by the total volume of regions with CT values  $> 500$  HU, which was defined as the threshold to detect calcified plaques based on the results of previous studies with intravascular imaging[6–8]. The present study demonstrated that a CACS  $\geq 162$  or CPV  $\geq 20.2$  mm<sup>3</sup> was a superior predictor for identifying the presence of CNs. Furthermore, recent OCT studies have demonstrated that the maximal calcium arc and thickness on cross-sectional analysis were larger in lesions with CNs than that of those without CNs[16–18]. Therefore, the calcified plaque area can be considered as a useful predictor

for the presence of CNs. The fact that AUC in MCPA was the highest among all the tested CCTA parameters and all the CNs were observed within calcified plaques with MCP support the usefulness of measuring MCPA for identifying the calcified lesions, including CNs.

This study also demonstrated that vessels with CNs had larger NCPV, LAPV, and calcium burden than that of those without CNs. These observations were consistent with the previous results of intravascular imaging[23, 24] and pathological studies[25]. In a sub-analysis of the PROSPECT study carried out using IVUS, Xu et al. reported that the coronary vessels in patients with CNs had a more necrotic core, thick-cap fibroatheroma, and dense calcium than that of those without CNs[24]. In the sub-analysis of CLIMA study[26], which is a large prospective registry on the plaque vulnerability assessed by OCT, Prati et al. reported that the patients with CNs showed coronary plaques with thinner fibrous cap in comparison to those without CNs. Furthermore, a pathological study on patients with sudden death due to acute coronary thrombosis caused by CNs revealed that the culprit arteries with CNs had more positive remodeling and larger plaque and calcification area than those arteries without CN[25]. These previous observations suggest that in addition to having a large calcium burden, coronary arteries with CNs also represent vulnerability and advanced atherosclerotic features.

Recent intravascular imaging studies have shown the association between calcified lesions with CNs and higher stent failure rates in patients who underwent newer-generation DES and modern devices[4, 5, 27]. Moreover, Prati et al. reported that the presence of CNs in non-culprit coronary plaques was associated with worse clinical outcomes, including cardiac death and target-vessel MI[26]. Hence, calcified lesions with CNs can be considered high-risk lesions. There is no established treatment for improving the clinical outcomes after PCI in calcified lesions with CNs and to prevent CNs-associated future coronary events; however, proper diagnosis of CNs is essential to stratify coronary events risks. To the best of our knowledge, the present study is the first to examine the CCTA predictors of OCT-detected CNs.

## Study limitations

This study had some limitations; first, the sample size was small, with only 11 patients in the CN group. Second, a potential selection bias exists as patients who underwent both the CCTA and OCT evaluations were included. At Nara Medical University, CCTA is generally avoided in patients with severe renal dysfunction, not on dialysis, and in unstable conditions, such as cardiogenic shock or congestive heart failure. Third, OCT assessments after pre-dilatation using a balloon catheter, rotational atherectomy, or thrombectomy were performed in about 20% of cases with severe narrowing not amenable to OCT or OFDI catheter passage or removal of blood from the field of view, which may have affected the visualization of the calcified plaques. Fourth, multivariate analysis of predictors of CNs could not be performed because of the small number of patients with CNs. Fifth, overestimation of CPV or MCPA due to partial volume effect and blooming artifact is inevitable. Therefore, a large-scale study is needed to verify the results of this study.

## Conclusions

CCTA is useful for predicting OCT-detected CNs in PCI target vessels, and quantitative measurements of the calcium burden in coronary vessels can help to identify the presence of CNs.

## Declarations

### Data availability statement

The datasets generated or analysed during the current study are available from the corresponding author on reasonable request.

### Acknowledgements

Authors thank the patients, participating cardiologists, and the staff who contributed to this study.

### Author contributions

J.S. wrote the main manuscript text and prepared the Figures. All authors, mainly M.W., reviewed the manuscript.

### Competing interests

The authors declare no competing interests.

## References

1. Virmani, R., Kolodgie, F. D., Burke, A. P., Farb, A. & Schwartz, S. M. Lessons from sudden coronary death: a comprehensive morphological classification scheme for atherosclerotic lesions. *Arterioscler. Thromb. Vasc. Biol.* **20**, 1262–1275 (2000).
2. Jia, H. *et al.* In vivo diagnosis of plaque erosion and calcified nodule in patients with acute coronary syndrome by intravascular optical coherence tomography. *J. Am. Coll. Cardiol.* **62**, 1748–1758 (2013).
3. Sugiura, J. *et al.* Progression of a calcified nodule causing acute myocardial infarction in a patient on hemodialysis – serial optical coherence tomography. *Circ. J.* **83**, 490 (2019).
4. Morofuji, T. *et al.* Clinical impact of calcified nodule in patients with heavily calcified lesions requiring rotational atherectomy. *Catheter. Cardiovasc. Interv.* **97**, 10–19 (2021).
5. Iwai, S. *et al.* Prognostic impact of calcified plaque morphology after drug eluting stent implantation – an optical coherence tomography study. *Circ. J.* **85**, 2019–2028 (2021).
6. Komatsu, S. *et al.* Detection of coronary plaque by computed tomography with a novel plaque analysis system, ‘Plaque Map’, and comparison with intravascular ultrasound and angioscopy. *Circ. J.* **69**, 72–77 (2005).
7. Soeda, T. *et al.* Diagnostic accuracy of dual-source computed tomography in the characterization of coronary atherosclerotic plaques: comparison with intravascular optical coherence tomography. *Int.*

- J. Cardiol. **148**, 313–318 (2011).
8. Soeda, T. *et al.* Intensive lipid-lowering therapy with rosuvastatin stabilizes lipid-rich coronary plaques. –Evaluation using dual-source computed tomography. *Circ. J.* **75**, 2621–2627 (2011).
  9. Sugiura, J. *et al.* Clinical course of optical coherence tomography-detected lipid-rich coronary plaque after optimal medical therapy. *Circ Rep.* **4**, 29–37 (2022).
  10. Agatston, A. S. *et al.* Quantification of coronary artery calcium using ultrafast computed tomography. *J. Am. Coll. Cardiol.* **15**, 827–832 (1990).
  11. Budoff, M. J. *et al.* Long-term prognosis associated with coronary calcification: observations from a registry of 25,253 patients. *J. Am. Coll. Cardiol.* **49**, 1860–1870 (2007).
  12. Detrano, R. *et al.* Coronary calcium as a predictor of coronary events in four racial or ethnic groups. *N. Engl. J. Med.* **358**, 1336–1345 (2008).
  13. Kataiwa, H., Tanaka, A., Kitabata, H., Imanishi, T. & Akasaka, T. Safety and usefulness of non-occlusion image acquisition technique for optical coherence tomography. *Circ. J.* **72**, 1536–1537 (2008).
  14. Kume, T. *et al.* Visualization of neointima formation by optical coherence tomography. *Int. Heart J.* **46**, 1133–1136 (2005).
  15. Sugawara, Y. *et al.* Plaque modification of severely calcified coronary lesions by scoring balloon angioplasty using lacrosse non-slip element: insights from an optical coherence tomography evaluation. *Cardiovasc. Interv. Ther.* **34**, 242–248 (2019).
  16. Kume, T. *et al.* Assessment of the coronary calcification by optical coherence tomography. *EuroIntervention* **6**, 768–772 (2011).
  17. Lee, T. *et al.* Prevalence, predictors, and clinical presentation of a calcified nodule as assessed by optical coherence tomography. *JACC Cardiovasc. Imaging* **10**, 883–891 (2017).
  18. Sugiyama, T. *et al.* Calcified plaques in patients with acute coronary syndromes. *JACC Cardiovasc. Interv.* **12**, 531–540 (2019).
  19. Finck, T. *et al.* Long-term prognostic value of morphological plaque features on coronary computed tomography angiography. *Eur. Heart J. Cardiovasc. Imaging* **21**, 237–248 (2020).
  20. Andreini, D. *et al.* Coronary plaque features on CTA can identify patients at increased risk of cardiovascular events. *JACC Cardiovasc. Imaging* **13**, 1704–1717 (2020).
  21. Lee, S. E. *et al.* Differences in progression to obstructive lesions per high-risk plaque features and plaque volumes with CCTA. *JACC Cardiovasc. Imaging* **13**, 1409–1417 (2020).
  22. Watanabe, M. *et al.* Side branch complication after a single-stent crossover technique: prediction with frequency domain optical coherence tomography. *Coron. Artery Dis.* **25**, 321–329 (2014).
  23. Fujii, K. *et al.* Expert consensus statement for quantitative measurement and morphological assessment of optical coherence tomography. *Cardiovasc. Interv. Ther.* **35**, 13–18 (2020).
  24. Xu, Y. *et al.* Prevalence, distribution, predictors, and outcomes of patients with calcified nodules in native coronary arteries: a 3-vessel intravascular ultrasound analysis from Providing Regional

Observations to Study Predictors of Events in the Coronary Tree (PROSPECT). *Circulation* **126**, 537–545 (2012).

25. Torii, S. *et al.* Eruptive calcified nodules as a potential mechanism of acute coronary thrombosis and sudden death. *J. Am. Coll. Cardiol.* **77**, 1599–1611 (2021).
26. Prati, F. *et al.* Clinical outcomes of calcified nodules detected by optical coherence tomography: a sub-analysis of the CLIMA study. *EuroIntervention* **16**, 380–386 (2020).
27. Watanabe, Y. *et al.* Comparison of clinical outcomes of intravascular ultrasound-calcified nodule between percutaneous coronary intervention with versus without rotational atherectomy in a propensity-score matched analysis. *PLOS ONE* **15**, e0241836 (2020).

## Figures

Figure 1. Study flow chart

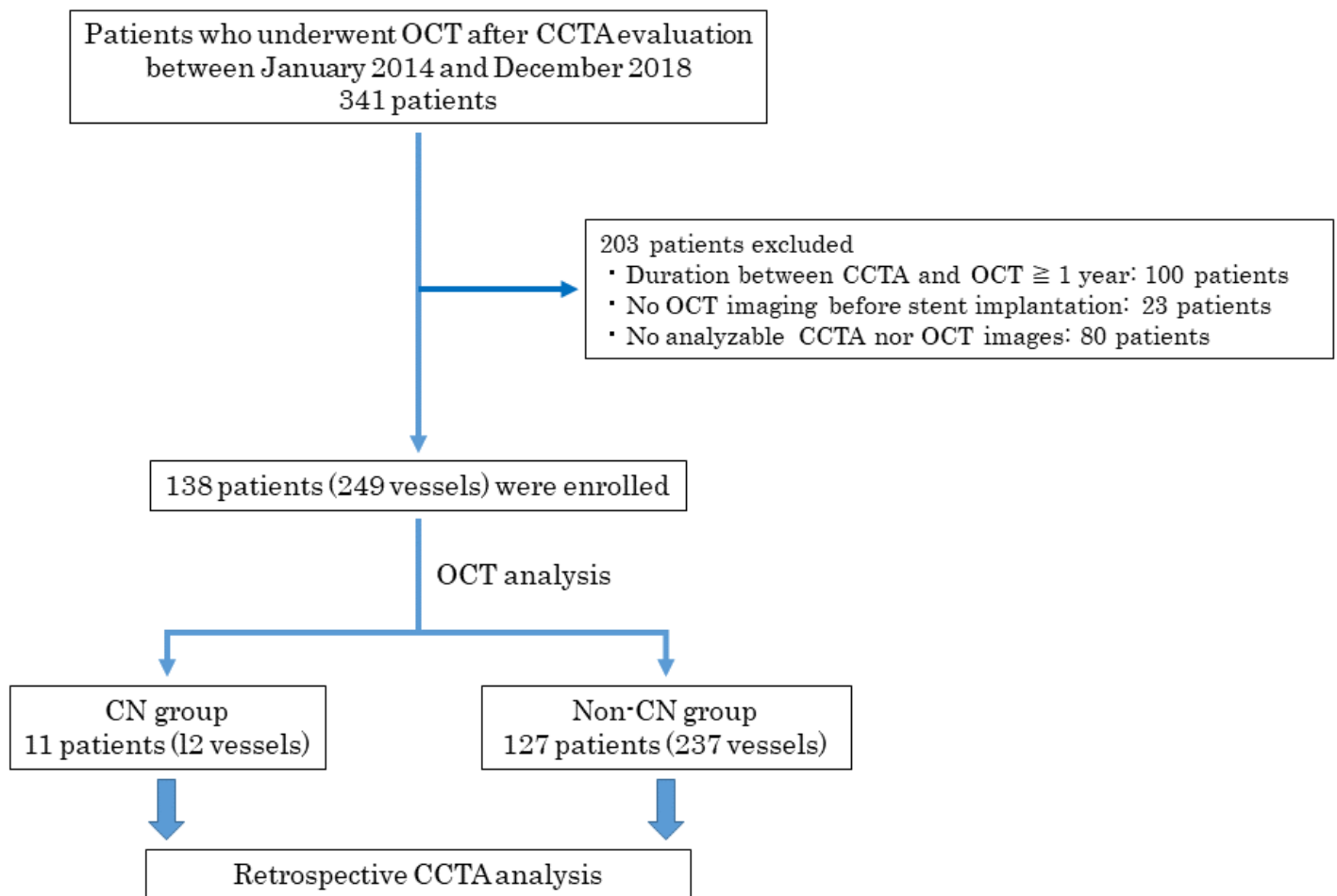


Figure 1

### Study flow chart

CCTA, coronary computed tomography angiography; CN, calcified nodule; OCT, optimal coherence tomography

Figure 2. Representative CCTA and OCT images of calcified plaques

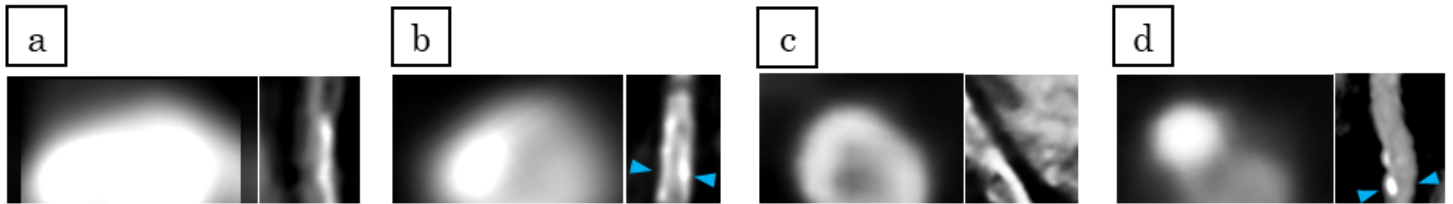


Figure 2

### Representative CCTA and OCT images of calcified plaques

- a. A representative image of calcified nodule. CCTA image showing a large area of calcification. The area of calcified plaque on the cross-sectional image (at blue arrow heads) is 21.77 mm<sup>2</sup>. The OCT image of this lesion demonstrates calcified nodules (plus symbols).
- b. A representative image of eccentric calcified plaque. The area of calcified plaque on the cross-sectional image (at blue arrow heads) is 2.8 mm<sup>2</sup>. The OCT image of this lesion demonstrates a superficial calcific sheet (asterisks).
- c. A representative image of circumferential calcified plaque. CCTA image showing a circumferential calcification. The area of calcified plaque on the cross-sectional image (at blue arrow heads) is 3.8



mm<sup>2</sup>. The OCT image of this lesion demonstrates a circumferential calcification (white arrow heads).

d. A representative image of spotty calcification. CCTA image showing a spotty calcification. The area of calcified plaque on the cross-sectional image (at blue arrow heads) is 0.8 mm<sup>2</sup>. The OCT image of this lesion demonstrated superficial small calcification (white arrow head).

CCTA, coronary computed tomography angiography; OCT, optimal coherence tomography

**Figure 3. ROC curve analysis for CCTA parameters to predict CN; CACS (a), CPV (b), NCPV (c), LAPV (d), MCPA (e)**

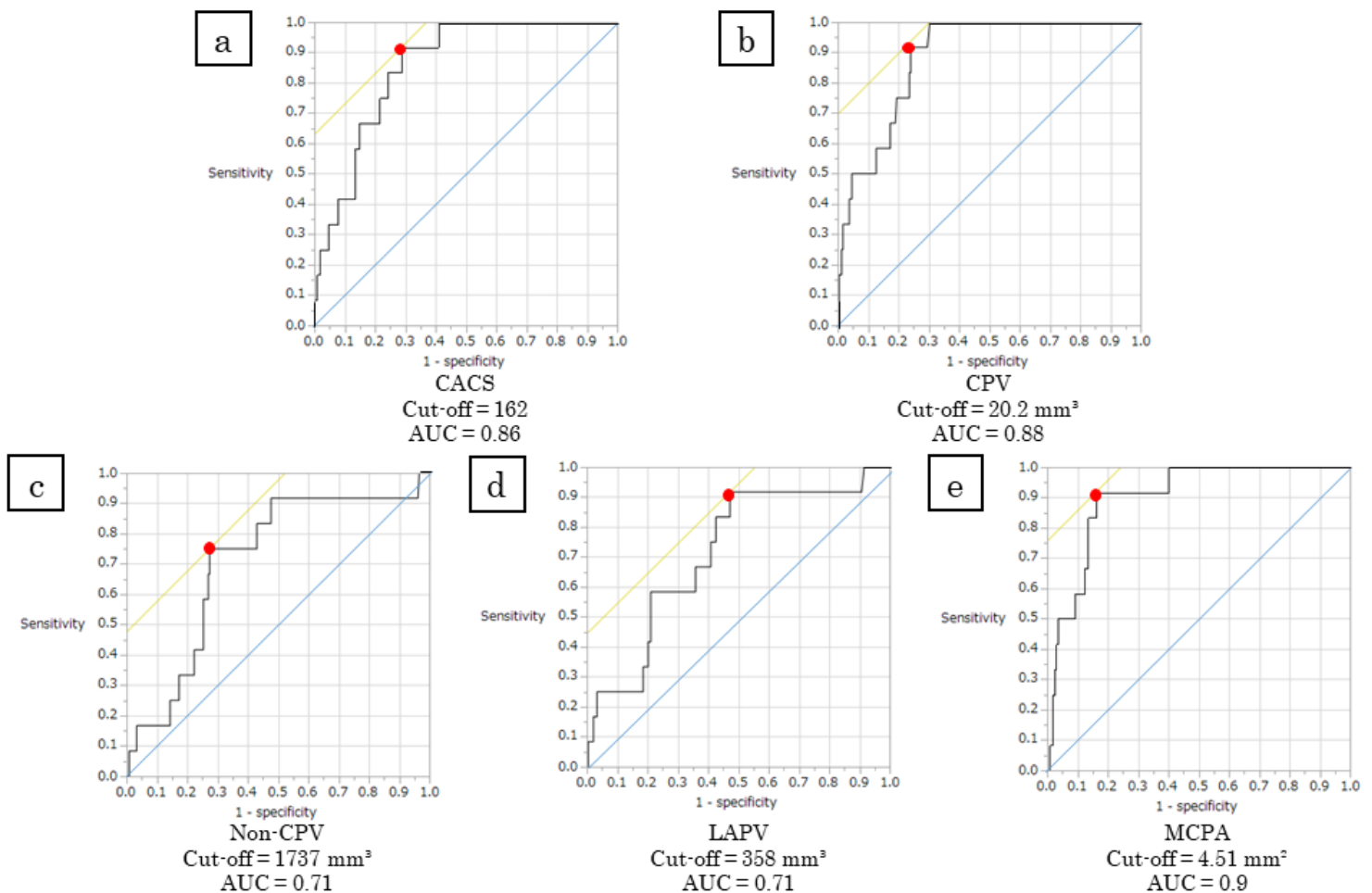


**Figure 3**

**ROC curve analysis for CCTA findings to predict CN; CACS (a), CPV (b), NCPV (c), LAPV (d), MCPA (e).**

The optimal cutoffs to predict CNs are CACS  $\geq 162$  (AUC = 0.86), CPV  $\geq 20.2$  mm<sup>3</sup> (AUC = 0.88), NCPV  $\geq 1737$  mm<sup>3</sup> (AUC = 0.71), LAPV  $\geq 358$  mm<sup>3</sup> (AUC = 0.71), and MCPA  $\geq 4.51$  mm<sup>2</sup> (AUC = 0.9).

AUC, area under the curve; CACS, coronary artery calcification score; CCTA, coronary computed tomography angiography; CN, calcified nodule; CPV, calcified plaque volume; LAPV, low-attenuation

plaque volume; MCPA, maximum calcified plaque area on cross-sectional image; NCPV, non-calcified plaque volume; ROC, receiver operating characteristic curve

## Supplementary Files

This is a list of supplementary files associated with this preprint. Click to download.

- [SupplementarymaterialScientificReportsScientificreports.docx](#)